International Journal of Applied Pharmaceutics

ISSN- 0975-7058 Vol 16, Issue 6, 2024

Original Article

FORMULATION, CHARACTERIZATION AND OPTIMIZATION OF PLGA-CHITOSAN-LOADED FATTY ACID SCAFFOLDS FOR THE TREATMENT OF DIABETIC WOUNDS

SHILPA N. THUMBOORU[1], SYED SUHAIB AHMED[1], BALAJI HARI[2], GOWRAV MP[3], KARRI VVS NARAYANA REDDY[1*]

[1]Department of Pharmaceutics, JSS College of Pharmacy, JSS Academy of Higher Education and Research, Ooty, Nilgiris, Tamil Nadu, India. [2]Department of Pharmacognosy, JSS College of Pharmacy, JSS Academy of Higher Education and Research, Ooty, Nilgiris, Tamil Nadu, India. [3]Department of Pharmaceutics, JSS College of Pharmacy, JSS Academy of Higher Education and Research, Mysuru, Karnataka, India
*Corresponding author: Karri Vvs Narayana Reddy; *Email: ksnreddy87@gmail.com

Received: 19 May 2024, Revised and Accepted: 29 Aug 2024

ABSTRACT

Objective: The objective of the current research to formulate Eicosapentanoic Acid/Decosahexanoic Acid (EPA/DHA)incorporated into Chitosan (CS)and Poly-Lactic-Glycolic Acid (PLGA), nanoparticles composite scaffolds to the accelerated diabetic wound healing. The main focus of this present research is to evaluate and develop the chitosan–PLGA biodegradable polymer scaffolds loaded with long-chain omega-3 Polyunsaturated Fatty Acids (PUFA's) (EPA/DHA).

Methods: Nano scaffolds were prepared by solvent evaporation method loaded with CS-PLGA, EPA and DHA to treat diabetic wounds at targeted site as pharmacotherapeutically. Upon investigation, the developed biodegradable crosslinked scaffold possesses matrix degradation, optimal porosity, prolonged drug release action than the non-cross linked scaffold. The prepared formulation containing CS-PLGA loaded with EPA/DHA were formulated as nanoscaffold for wound topical applications was carried out by using freeze drying process.

Results: The prepared CS-PLGA nano scaffolds were optimized and evaluated for physicochemical properties, dynamic light scattering with a particle size of 248 nm and zeta of-24mVand Scanning Electron Microscopy (SEM) were found to be spherical. In addition, the optical properties of EPA/DHA and PLGA, along with CS, can be compared by examining their absorption and wavelength (nm) using UV-visible spectroscopy. The structural and functional groups of the prepared end products were characterized by Fourier-Transformed Infrared Spectroscopy (FT-IR) has shown good compatibility with excipients and nanoformulaton, *in vitro* drug release studies done by using dialysis bag membrane results find that first-order Higuchi model was followed showing 20% release in first 0.2 h. MTT(3-(4,5-dimethylthiazolyl)-2,5-diphenyltetrazolium bromide) assay was carried out and it showed that both crosslinked and non-crosslinked scaffolds(110 and 120%) improved cell growth when compared to control (100%).

Conclusion: Finally, the results showed that the PLGA, CS nanoscaffolds containing 98% of PUFA's (EPA/DHA) have increased in proinflammatory cytokines production at the particular wound site and thus accelerated healing activity, depending on the pre-clinical studies have trespassed, the therapeutic potential to penetrating at wound site. The optimized nanoformulation could be a better formulation for targeting and treatment of diabetic wounds at an optimal ratio.

Keywords: PUFAs, Chitosan, Scaffolds, PLGA, Diabetes, Wounds, *In vitro* drug release, *In vitro* studies

DOI: https://dx.doi.org/10.22159/ijap.2024v16i6.51509 Journal homepage: https://innovareacademics.in/journals/index.php/ijap

INTRODUCTION

According to the International Diabetic Federation (IDF), the prevalence of diabetic injuries in 2019 is between 98 to 327 million (in 2017) and 191 to 438 million (in 2045) in people aged 65 to 79 y (older people) and people aged 20 to 64 y (adults). The chronic wounds in diabetics are 70% for every 30 sec, and the lower leg is lost to foot amputations [1]. Patients who typically suffer from delayed wound healing require innovative techniques and novel strategies that must be considered to solve this problem. Diabetic wounds are a major cause of mortality among individuals with diabetes. Standard care therapies for treating diabetic wounds include patient education, blood glucose control, wound debridement, off-loading, surgery, and advanced therapies. Currently, diabetic wound treatment focuses on early diagnosis, prevention, and patient education. The pathogenesis of diabetic wound healing is multifactorial, with long-term inflammation, infections, and improper tissue management being the primary factors impairing wound healing [2]. Active dressings that have emerged are aimed at either controlling infection by delivering antimicrobials or modifying Matrix Metalloproteinase (MMP) levels at the wound site. The constantly flourishing field of biomaterials and tissue regeneration research has contributed to the evolution of novel materials to be incorporated for the treatment of various morbid circumstances. Based on the above literature, in this current research, Eicosapentanoic Acid/Decosahexanoic Acid (EPA/DHA) loaded Poly-Lactic-Glycolic Acid (PLGA) and chitosan (CS) nanoparticles were fabricated and incorporated into scaffolds to reduce inflammation and promote tissue regeneration in infected diabetic wounds [3]. Furthermore, incorporating EPA/DHA into PLGA-CS nanoparticles within nanohybrid scaffolds improves the physical attributes, corrosion rate, and biodegradation of the composite scaffolds. These scaffolds serve as drug depots for enhanced controlled release of EPA, DHA, and PLGA-CS NPs. This scaffold not only minimizes inflammation and infections but also aids in enhancing cell proliferation and tissue regeneration in diabetic wounds. Fatty acids have pathological and physiology roles in different types of diseases such as atherosclerosis, inflammation (or) normal wound healing; the outcome of fatty acids on wound healing is through repairs in plasma membrane properties, such as changes in phospholipids compositions, which also increased in the activity of growth factor and having decreased in eicosanoids production. The fatty acids EPA/DHA are rich sources of omega-3 fatty acids that have many potential effects on modulating various diseases, especially in diabetic patients, and improve vasodilator properties [4].

NPs have been utilized using unique properties on their surface such that the porosity of cross-linked and noncross-linked scaffolds could be increased. Because chitosan includes a hydrophilic hydroxyl group, chitosan interacts with water molecules-Such as hydrogen bonds easily and concurrently; PLGA is a useful coating material that is frequently employed to improve the stability and solubility of hydrophobic substances and due to its good biocompatibility and

biodegradability. However, because PLGA NPs have a negatively charged surface, it is not ideal for absorption and digestion [5]. In contrast, CS improves the physical and chemical properties of PLGA NPs. In this present research work, EPA/DHA PLGA-CS NPs were prepared by freeze-drying method as a composite carrier for EPA/DHA delivery [6, 7]. These NPs characteristics were determined by Fourier Transformed Infrared Spectroscopy (FT-IR), DSC, and SEM. Lastly, by improving the EPA/DHA PLGA-CS, NPs can continuously protect and transport the EPA/DHA by enhancing the solubility, entrapment efficiency, storage stability and controlled release effect of EPA/DHA. To develop EPA/DHA loaded PLGA-CS NPs in diabetic wound healing scaffold matrix formulation our proposed hypothesizes (fig. 1) that selective n-3 PUFA, EPA, and DHA NPs loaded cs scaffolds applied topically elicit anti-inflammatory and anti-microbial activities effectively in diabetic wound sites.

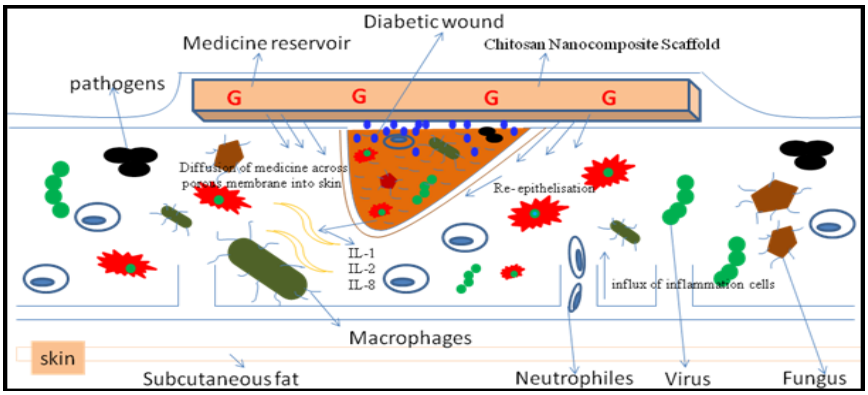

Fig. 1: Factor considerations of the diabetic wounds and formulation design, some of the growth factors affect the wound site to fight against the inflammatory cells and anti-microbial infections [image was created by using Biorender software]

MATERIALS AND METHODS

Materials

PLGA was procured from Nomisma Healthcare®, India. EPA® and DPA® were purchased from Thermo Scientific Chemicals. Chitosan was procured from Sisco® research laboratories, and 3T3 l-1 fibroblast cell lines were procured from NCCS Pune, India.

Preparation of CS scaffolds

EPA/DHA PLGA NPs were prepared using the anti-solvent method as a composite carrier for DHA delivery, with modifications from our previous studies. Dissolve 1 ml EPA/DHA and 25 mg PLGA in 3.5 ml of acetone and sonicated for 15 sec to form oil phase a-solution; then, A liquid was slowly dispersed into 15 ml water phase at a flow rate of 2 ml/min (dropwise) to obtain B-liquid. Homogenization of the B-Solution was done using IKA T-18 Ultra Turrax homogenizer (IKA, Wilmington, NC, USA) at 15,000 rpm and 400 watts at the same temperature for 25 min and ultrasonicated using a high-intensity probe ultrasonic processor (60 W) and stirred in a cold-water bath (4 °C) with a magnetic force of 2000 rpm for 20 min. Then, the formed nano-emulsion was continuously magnetically stirred for 24 h to evaporate the acetone [8]. The obtained nano-emulsion was washed 3 times by ultrafiltration to obtain PDNP samples and stored in a refrigerator at 4 °C for reserved. The preparation procedure of blank PLGA-NPs was the same as above without EPA/DHA.

Preparation of PLGA-CS NPs and PLGA-CS Loaded EPA/DHA NPs

CS was coated onto PLGA NPs through an electrostatic interaction force. Specifically, 1 mg/ml CS solution (1% acetic acid) and the PLGA NPs mixture (Ultrasound in advance, 60w, min) were added dropwise to the CS solution. After 30 min of magnetic stirring, PLGA-CS solution (1000rpm/min) was obtained. The remaining samples were stored in the freeze-dried to obtain PLGA-CS NPs. To the above solution, the EPA/DHA PLGA NPs were added to the solution (ultrasound in advance, 60 w, 1 min) dropwise to the CS solution with 1 mg/ml and then stirred for 1h (1000rpm/min) Half of the samples were stored in a refrigerator at 4 °C, the other sample was freeze-dried to obtain EPA/DHA PLGA-CS NPs [9, 10].

Statistical experimental design

The optimization of the formulation was conducted using Design-Expert software (Design Expert 13, Stat Ease Inc., Minneapolis, USA). PLGA concentration (X1), chitosan concentration (X2), and homogenization speed (X3) were selected as independent variables. These variables were assigned low, medium, and high values based on their significant impact on Critical Material Attributes (CMAs), such as particle size (Y1) and entrapment efficiency (Y2). The coded values of the independent variables are listed in table 1. This design aimed to explore the main effects of independent variables and their potential interactions on formulation characteristics to maximize entrapment efficiency and minimize particle size. The Box-Behnken design was chosen for its efficiency and requirement of fewer runs compared to the central composite design. *ANOVA* test was employed for statistical validation and to generate polynomial equations using the Design-Expert software [11].

The responses obtained from the input variables were fitted into different models, including linear, quadratic, cubic, and 2FI. Significance was determined based on a P-value below 0.05. Design-Expert software facilitated the generation of 3D response plots by conducting a comprehensive grid search across the experimental region. Experimental values were quantitatively compared to the predicted values obtained from these response plots. Data analysis was performed using Design-Expert software to derive polynomial equations, and model evaluation included assessing statistical coefficients and R^2 values. Three-dimensional (3D) surface plots were utilized to visually represent the relationships between variables and responses.

Table 1: Variables and their levels for preparation of EPA/DHA PLGA-CS NPs

Variables				Level of variables	
Independent variables (Uncoded)	**Coded**	**Coded level**	**Low**	**Medium**	**High**
PLGA (mg/ml)	A	-1	10	20	30
Chitosan (%w/v)	B	0	1	1.5	2
Homogenization speed (RPM)	C	1	6000	9000	12000
Dependent factors			Constraints		
Particle size(nm) (Y_1)			Minimum		
Entrapment efficiency (%) (Y_2)			Maximum		

Determination of particle size, zeta potential and polydispersity index

All samples were diluted 1:10 with Millipore water and filtered through a 0.45 µm membrane filter to achieve optimal counts. Particle size, zeta potential, and PDI were determined using an Anton Paar Litesizer 500 (Malvern Instruments, UK) with cmPALS technology at a scattering angle of 90°. The diluted dispersion was introduced into a polystyrene cuvette with a 10 mm path length and allowed to equilibrate for 120 sec [12].

Determination of drug entrapment efficiency

The entrapment efficiency of EPA/DHA PLGA-CS NPs was evaluated using the centrifugation technique. A 15 ml dispersion of NPs was centrifugated at 17,000 rpm for 30 min at room temperature using equipment from Remi Instruments Pvt. Ltd, India. The percentage of entrapment efficiency (%EE) was determined by calculating the difference between the total drug used in nanoparticle preparation and the amount of drug found in the supernatant. The drug concentration in the supernatant was measured at λmax 250 nm using a Shimadzu 1800 UV-spectrophotometer [13].

$$\% \text{ Entrapment efficiency} = \frac{\text{total drug} - \text{free drug}}{\text{total drug}} \text{x } 100$$

FTIR spectroscopy analysis

FTIR spectroscopy of CS-PLGA, EPA, DHA, CS-PLGA-EPA, and CS-PLGA-DHA was conducted using a Nicolet iS10 FTIR spectrophotometer with a resolution of 2 cm^{-1} over 64 scans. A thin plate of potassium bromide was used as a background. In summary, a 2.0 mg freeze-dried sample was mixed with 198 mg pure potassium bromide (KBr) powder. The mixture was then pressed into a pellet and analyzed by FTIR in the range of 400–4000 cm^{-1} [14].

Morphological determination by SEM

The surface morphology of NPs was observed using the Shimadzu S4800 instrument through SEM analysis. The sample processing method and device parameter settings were consistent with those described in our previously reported literature. In brief, a thin layer of gold was applied to the particles to enhance SEM visualization. Images were captured using an electron beam acceleration voltage ranging from 10 to 15 kV [15].

Porosity

The porosity of both cross-linked CS-PLGA-EPA and CS-PLGA-DHA and non-cross-linked scaffolds were determined using the liquid displacement method. Ethanol was chosen as the displacement liquid due to its ability to permeate the scaffold pores effectively without inducing contraction or swelling [16]. Porosity was calculated using the equation below:

$$\% \text{ porosity} = \frac{\text{Wwet} - \text{Wdry}}{\text{Vscaffold}} \text{X } 100$$

Where W indicates the weight of the scaffold and V denotes the volume of the scaffold.

Water absorption test

The initial weight (Wi) of both crosslinked and non-crosslinked scaffolds was recorded. Subsequently, the scaffolds were submerged in phosphate-buffered saline (PBS) at pH 7.4 and kept at 37 °C for 72 h. After removing the excess solvent by blotting, the weight (Ws) was measured. The scaffolds were then lyophilized to determine their water absorption capacity [17]. It was determined by using the following equation.

$$W_{ab} = \frac{[W_s - W_i]}{Wi} \text{X } 100$$

Where Wab represents the water absorption of the scaffold at equilibrium, and Wi and Ws denote the scaffold's dry and wet weights, respectively.

***In vitro* drug release study**

The preformed crosslinked and non-crosslinked composite scaffolds were submerged in 200 ml of Simulated Wound Fluid (SWF) at pH 7.4, kept at 37 °C with continuous stirring. Periodically, the supernatant was exchanged with an equal volume of fresh SWF, and the collected supernatant was filtered using a 0.2µm membrane filter. The quantity of crosslinked scaffold released from the scaffolds was quantified at 250 nm [18].

MTT assay

The MTT assay was conducted to assess the cell viability of composite scaffolds. 3T3-L1 fibroblast cell lines (Procured from NCCS, Pune, India)were seeded at a density of 5×10^3 cells per well in a 96-well plate and cultured in Dulbecco Modified Eagles Medium (DMEM) supplemented with 10% FBS for 24 h. The cells were then centrifuged, and the pellets were resuspended in wells containing 100 µL of CS-PLGA-EPA scaffold, CS-PLGA-DHA scaffold, placebo, control (cells in the medium), and blank (medium alone). The plates were then placed in a humidified CO_2 incubator at 37 °C for 48 h. Subsequently, 100 µl of MTT solution (1 mg/ml) was added to each well, and the plates were gently shaken and further incubated at 37 °C for 2 h. Formazan crystals formed were solubilized by adding 100 µl of DMSO, and the absorbance was measured at 570 nm using a microplate reader (ELx 800, Biotek®, CA)). The percentage of cell viability was calculated and compared with the blank and control samples [19].

RESULTS AND DISCUSSION

Optimization of scaffolds by box-behnken method

Thirteen experimental runs were generated using the Box-Behnken design in Design Expert software. These runs encompassed different levels (low, medium, high) of independent variables and responses aimed at optimizing key variables for nanoparticles to achieve small particle size and high entrapment efficiency. The linear model was identified as the best-fit for the dependent variables. Tables 2-5 depict the results of the 13 experimental runs for the cross-linked scaffolds, including regression analysis summaries for the responses and *ANOVA* for the response models (R1, R2).

Table 2: Observed responses of 13 run experimental designs according to box-behnkem design

Run	Factor 1	Factor 2	Factor 3	Response 1 (Y1)	Response 2 (Y2)
	A: PLGA conc (mg/ml)	B: Chitosan (% w/v)	C: Homogenization speed (rpm)	Particle size (nm)	Entrapment efficiency (%)
1	0	1	1	257±1.11	71.33±0.32
2	-1	-1	0	458±0.52	49.22±0.87
3	-1	1	0	311±0.33	63.22±0.23
4	-1	0	1	266±1.33	58.22±1.44
5	-1	0	-1	483±2.11	48.22±1.42
6	1	0	-1	599±1.33	54.22±0.58
7	0	1	-1	488±0.22	57.22±0.11
8	1	0	1	400±0.11	67.33±1.89
9	0	-1	1	410±0.43	52.27±1.43
10	1	1	0	446±1.21	69.22±1.56
11	1	-1	0	580±2.17	52.32±1.43
12	0	-1	-1	622±2.53	47.47±1.77
13	0	0	0	436±0.33	57.36±1.75

Value are in mean±SD, n=3

Effect on particle size

The experiments conducted across 13 runs yielded particle sizes ranging from 257 to 622 nm depending on the levels of independent factors. The factors influencing particle size included PLGA concentration (mg/ml), CS concentration (% w/v), and homogenization speed (rpm) ($p<0.001$, table 3 and fig. 2). In the polynomial equation, a positive sign indicates a synergistic relationship where variables interact positively, enhancing the combined effect. Conversely, a negative sign indicates an antagonistic relationship where variables interact negatively, diminishing the combined effect. The linear model was identified as the most suitable for describing the impact of particle size, which can be expressed using the following quadratic equation:

Particle size (Y1) =+439.21+69.57A-71.10B-113.65C .... Eq (1)

The model F-value of 186.68, with a significance level of $P<0.0001$, confirmed its statistical significance. Among the model terms, A (PLGA concentration) and B (CS concentration) were significant. The positive coefficient of A indicated a synergistic effect on particle size, while the negative coefficients of B and C (homogenization speed) indicated antagonistic effects. The predicted R^2 of 0.965138 correlates well with the adjusted R^2 of 0.97891. This close alignment indicates the model's suitability and reliability in predicting particle size. The 3-Dimensional (3D) response surface plots illustrated the influence of various formulation variables on particle size (Y1). The average particle size ranged from 257 to 622 nm, reflecting comprehensive effects. An increase in the solid lipid ratio and surfactant ratio led to an increase in particle size, while higher surfactant concentration and homogenization speed resulted in a reduction in particle size. The impact of particle size on different factors is depicted in fig. 2.

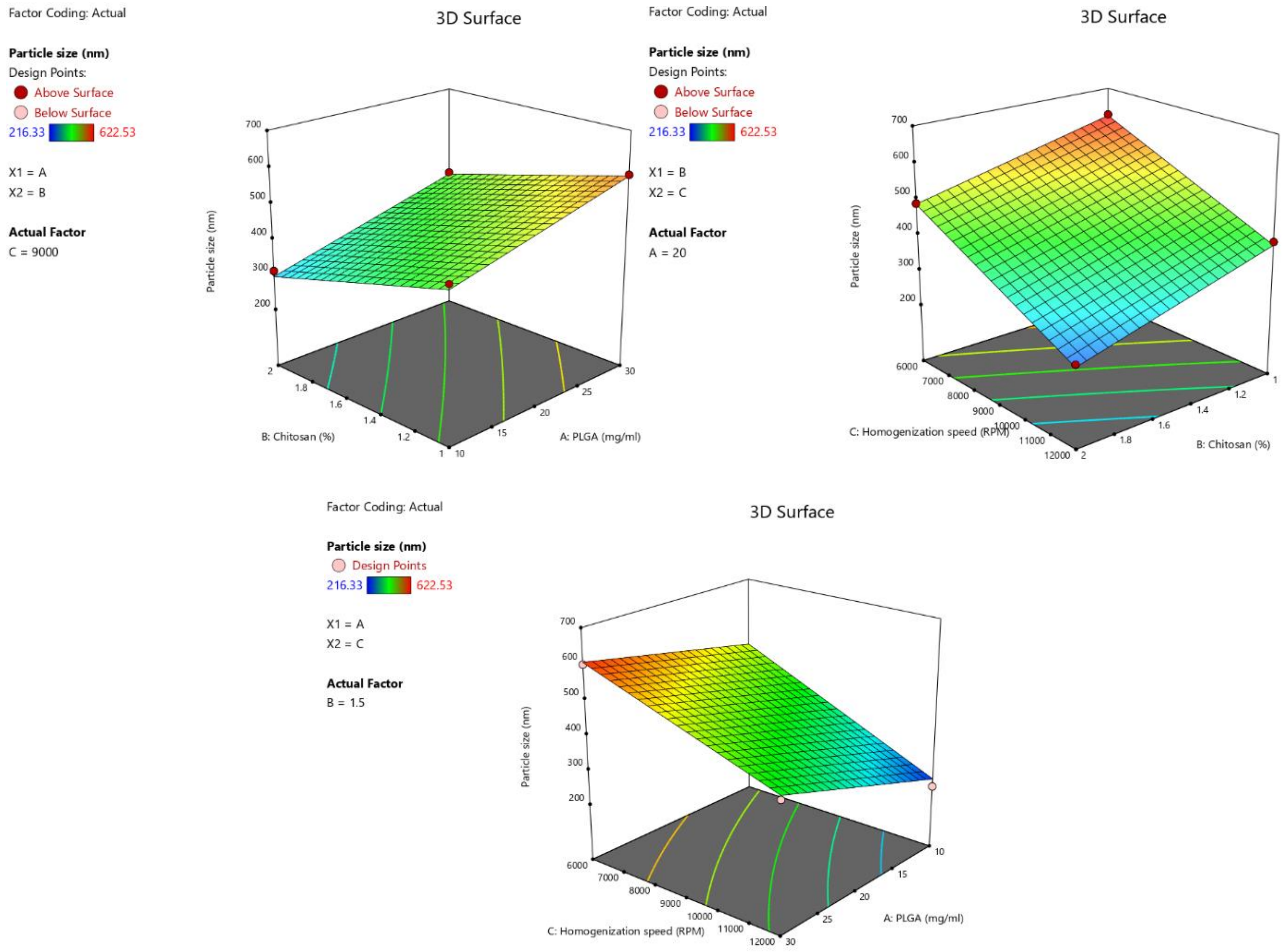

Fig. 2: 3D response plots showing the effect of independent variables on particle size

Effect on entrapment efficiency

The polynomial equation (Eq 2) demonstrates that all independent variables positively influence entrapment efficiency, as illustrated below.

EE(Y2) =+57.51+3.03A+7.46B+5.25C+0.7250AB+0.7775AC+2.33BC...Eq.(2)

The model exhibited a statistically significant F value of 58.97 ($P<0.0001$), indicating its significance. In this instance, model terms A, B, C, AB, AC, and BC were all found to be significant. Moreover, all coefficient variables demonstrated a positive effect, suggesting a synergistic influence. The linear model emerged as the most suitable for entrapment efficiency. The model effectively predicts entrapment efficiency with a predicted R^2 of 0.9692, close to the adjusted R^2 of 0.9854. Visualized through 3D response surface plots, the impact of various formulation variables on entrapment efficiency (Y2) is evident. Entrapment efficiency, ranging between 47% to 71.3%, demonstrated positive impacts as the solid lipid ratio and surfactant ratio increased. Likewise, higher surfactant concentration and homogenization speed correlated with increased entrapment efficiency. The effect of entrapment efficiency on various factors has been illustrated in fig. 3.

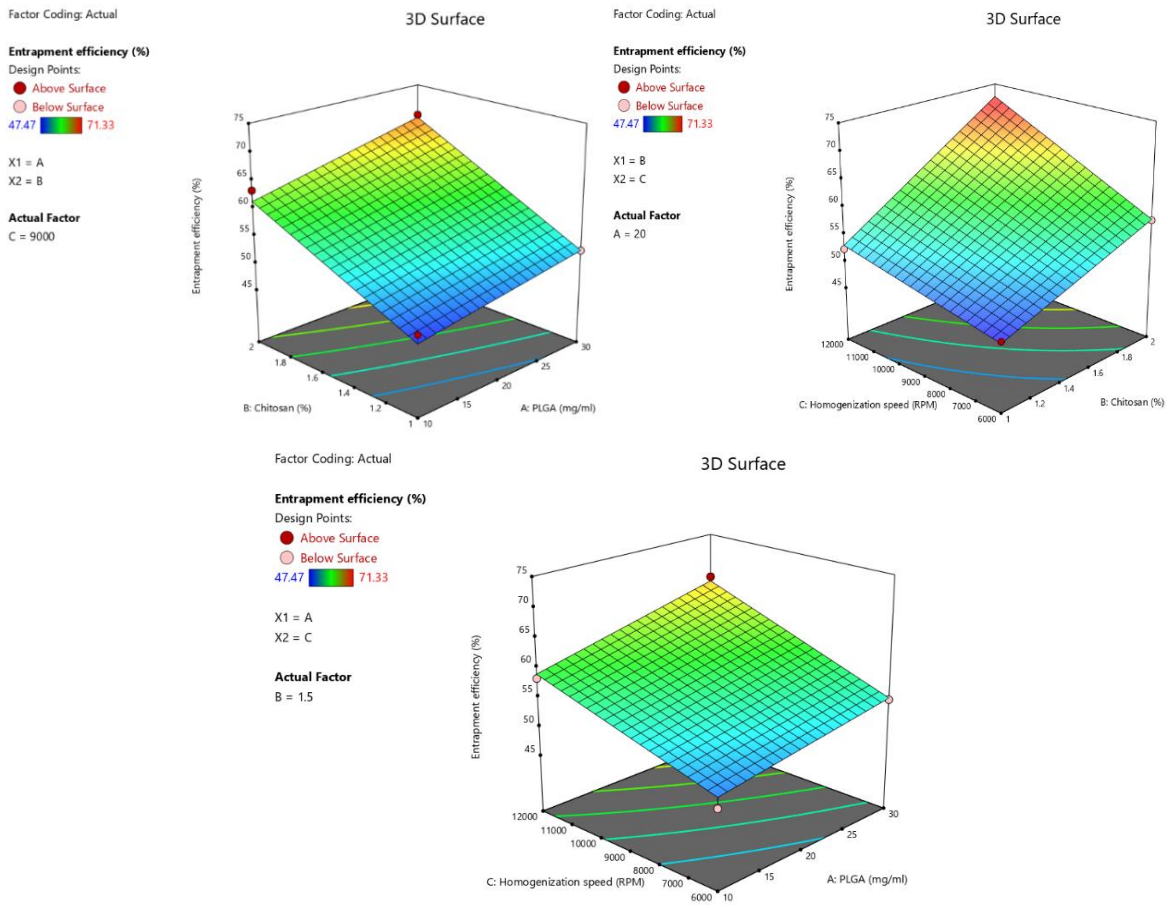

Fig. 3: 3D response plots showing the effect of independent variables on entrapment efficiency

Variable interaction and point prediction

Perturbation plots were employed to assess the degree of variation in independent variables and their corresponding responses. These plots revealed that an increase in PLGA and CS concentrations led to an increase in particle size. Conversely, an increase in CS concentration and homogenization speed resulted in an increase in particle size (fig. 4). While, the increase in PLGA and homogenization speed led to a decrease in particle size. Similarly, an increase in PLGA concentration and chitosan concentration led to a gradual increase in entrapment efficiency. An increase in CS concentration and homogenization speed led to steady increase in EE. Point prediction using Design Expert software was utilized to optimize both particle size and entrapment efficiency. The formulations that best met the criteria were selected and optimized to achieve minimal particle size and maximum entrapment efficiency. The low percentage prediction error values validated the obtained polynomial equations and demonstrated the applicability of response surface methodology (RSM). Therefore, the optimization provided values for PLGA as 16.2 mg, CS as 2%, and a homogenization speed of 12000 rpm. The estimated particle size and entrapment efficiency for the optimized scaffold were 254 nm and 70.89%, respectively [20].

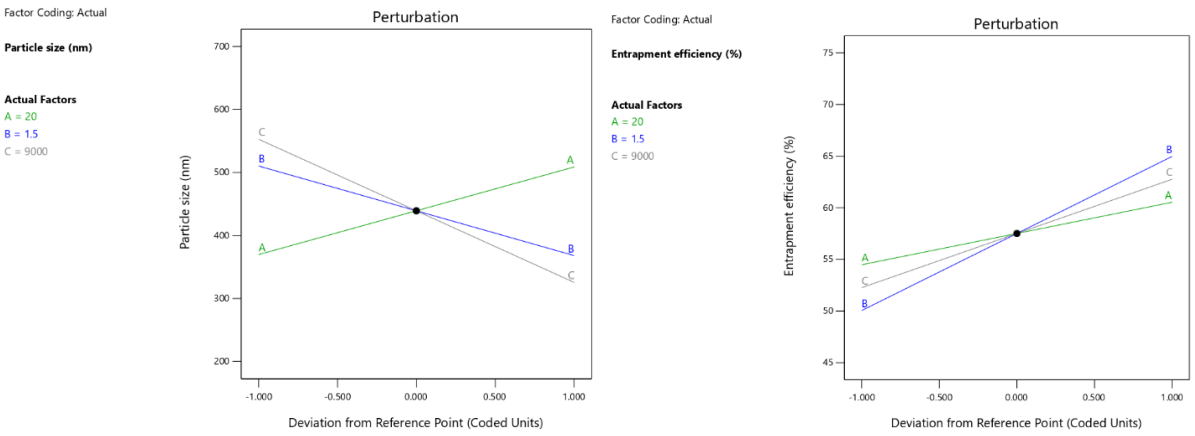

4(a) **4(b)**

Fig. 4: (a) perturbation plots on particle size, (b) Perturbation plots on entrapment efficiency

Table 3: Analysis of variance for the response particle size (R1)

Source	Sum of squares	df	Mean square	F-value	p-value	
Model	1.83E+05	3	60829.13	186.68	<0.0001	significant
A-PLGA	38715.71	1	38715.71	118.82	<0.0001	
B-Chitosan	40438.84	1	40438.84	124.1	<0.0001	
C-Homogenization speed	1.03E+05	1	1.03E+05	317.12	<0.0001	
Residual	2932.62	9	325.85			
Cor total	1.85E+05	12				

Table 4: Analysis of variance for the response entrapment efficiency (R2)

Source	Sum of squares	df	Mean square	F-value	p-value	
Model	765.83	6	127.64	58.97	<0.0001	significant
A-PLGA	73.27	1	73.27	33.85	0.0011	
B-Chitosan	445.66	1	445.66	205.92	<0.0001	
C-Homogenization speed	220.71	1	220.71	101.98	<0.0001	
AB	2.1	1	2.1	0.9715	0.3624	
AC	2.42	1	2.42	1.12	0.3312	
BC	21.67	1	21.67	10.01	0.0195	
Residual	12.99	6	2.16			
Cor total	778.81	12				

Table 5: Summary of the results of regression analysis of responses

Model	R^2	Adjusted R^2	Predicted R^2	Adequate precision	SD	% CV	Remark
Response (Y1)							
2FI	0.2985	0.9821	0.9503	31.1661	16.62	3.78	
Linear	0.0001	0.9789	0.9651	36.9017	18.05	4.11	Suggested
Response (Y2)							
Linear	0.069	0.9667	0.907	23.5589	1.47	2.56	Suggested
2 FI	0.0001	0.9329	0.889	21.9759	2.09	3.63	

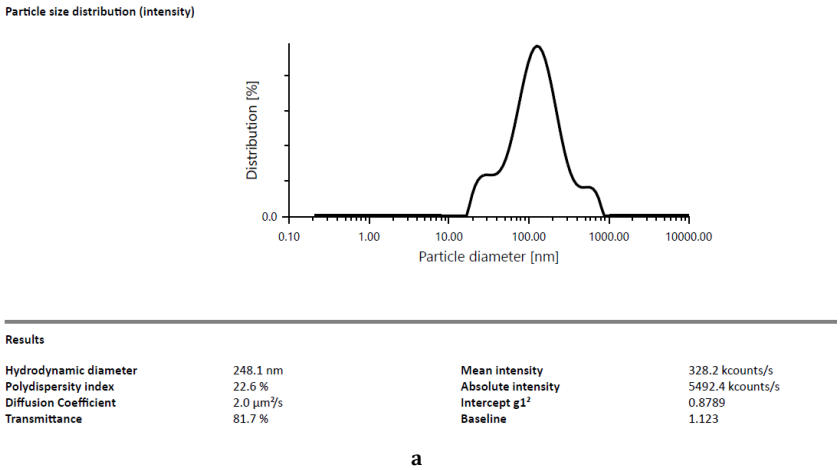

a

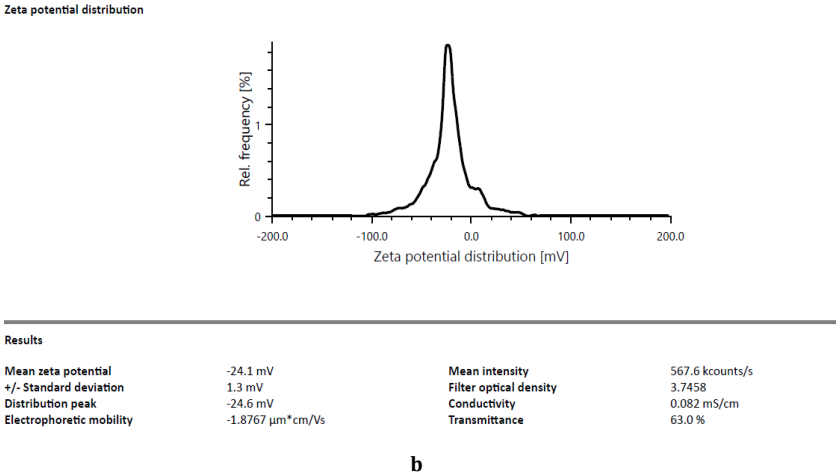

b

Fig. 5: (a) particle size of crosslinked scaffold (b) zeta potential of crosslinked scaffolds

Physicochemical characterization of cross-linked scaffolds

The optimized formulation particle size, Polydispersity index (PDI), and zeta potential are illustrated in fig. 5. The average particle size, PDI, and zeta potential were 223 nm, 0.203, and-20 mV, respectively. These results suggest that the narrow particle size distribution indicates consistency, uniformity, and stability of the formulation, while the zeta potential reveals good electrostatic interaction between nanoparticles [21].

Determination of entrapment efficiency (EE)

The EE of optimized DZN-FA SLNs and DZN SLNs was 72±2 % and 69±3% respectively.

FTIR analysis

The peaks for chitosan at 3585 cm^{-1},2977 cm^{-1},2233 cm^{-1},1695 cm^{-1},1524 cm^{-1} correspond to the presence of O-H, N-H, C≡C, C=O groups. The peaks for CS+PLGA at 3535 cm^{-1},2940 cm^{-1},1724 cm^{-1},1510 cm^{-1} correspond to the presence of the peaks for EPA at 3622 cm^{-1}, 1683 cm^{-1} correspond to the presence of O-H str, C=N str. The peaks for EPA at 3623 cm^{-1}, 3014 cm^{-1},1634 cm^{-1} correspond to the presence of O-H str, carboxylic str, N-H str, C=C str. The peaks for chitosan+PLGA+EPA at 3634 cm^{-1}, 2209 cm^{-1}, 1633 cm^{-1},1587 cm^{-1}correspond to the presence of O-H str, C≡C str, C=C str, N-H str. The peaks for Chitosan+PLGA+DHA at 3647 cm^{-1}, 2191 cm^{-1},1631 cm^{-1}, 1402 cm^{-1}correspond to the presence of O-H str, C=C str, C=C str, C-H str. Hence, formulated scaffolds were found to be compatible with the pure drug and excipients (fig. 6).

SEM

The prepared formulation was found to be spherical in shape, and the scaffolds were found to be spongy, porous arrangements. Crosslinked scaffolds were depicted in fig. 7.

Porosity and water absorption test

The porosity and water absorption of crosslinked and non-crosslinked scaffolds are represented in table 6. In crosslinked scaffolds, the diameter of pores was found to be in the range of 23.43-50.22 µm, whereas in the non-crosslinked it was found to be 36.33-63.22 µm. The crosslinked scaffolds had a mean pore size of 33.33 µm, and the non-crosslinked scaffolds had a mean pore size of 46.44 µm (table 6). As evidenced, the porosity of crosslinked scaffolds was lower compared to non-crosslinked scaffolds due to the formation of strong intermolecular interactions with the EPA and DHA of scaffolds, leading to the fusion of small pores to form larger ones. Water absorption refers to the ability of a scaffold to retain water, which is a vital factor in tissue engineering. The swelling property of crosslinked scaffold was relatively low compared to non-crosslinked scaffold, possibly due to hydrophilicity and retaining 3D structure.

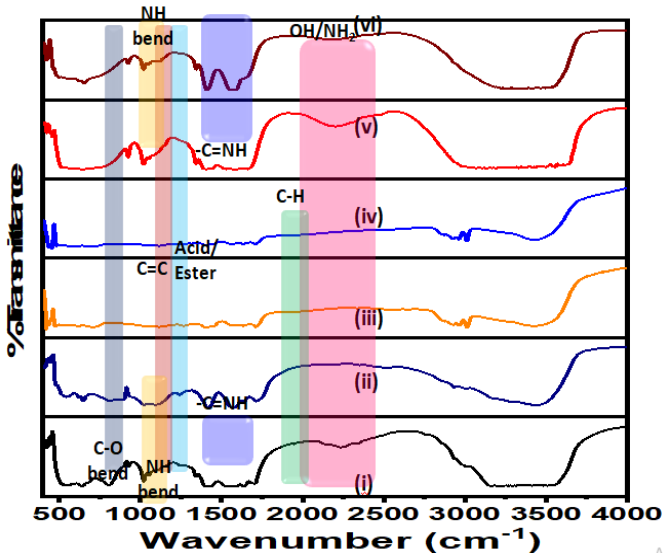

Fig. 6: (i) CS (ii)PLGA-CS, (iii) EPA, (iv) DHA, (v) CS-PLGA-EPA, (vi) CS-PLGA-DHA

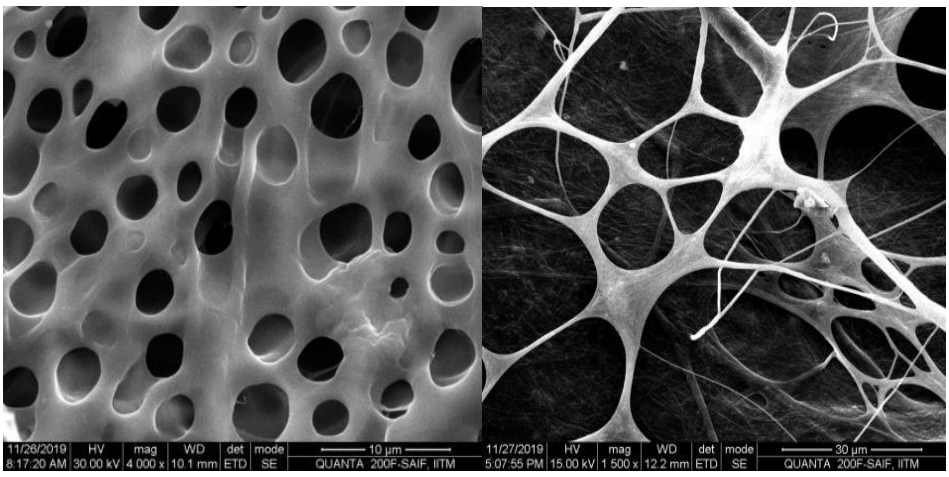

Fig. 7: Morphology of scaffolds of CS-PLGA-EPA and CS-PLGA-DHA by SEM

Table 6: % porosity and water absorption of crosslinked scaffolds

S. No.	Scaffold type	% Porosity	% Water absorption
1	Non-crosslinked scaffold	95.33±0.33	755±0.91
2	Crosslinked scaffold	74.22±1.22	475±1.33

Value are given in mean ±SD, n=3

In vitro drug release

In vitro drug release for crosslinked and non-crosslinked scaffolds initially showed a burst release followed by a sustained release pattern. Burst release may be due to solubility and penetration of water into the polymer matrix system. The drug latter followed a sustained pattern, which might be due to the coating of PLGA and CS polymer, thereby releasing from the inner core in a slow pattern. The crosslinked scaffolds exhibited slower drug release (55%) compared to non-crosslinked scaffolds (PLGA-CS) (85%). Hence, crosslinked scaffolds showed more ideal properties, such as porosity and water absorption (fig. 8) [22].

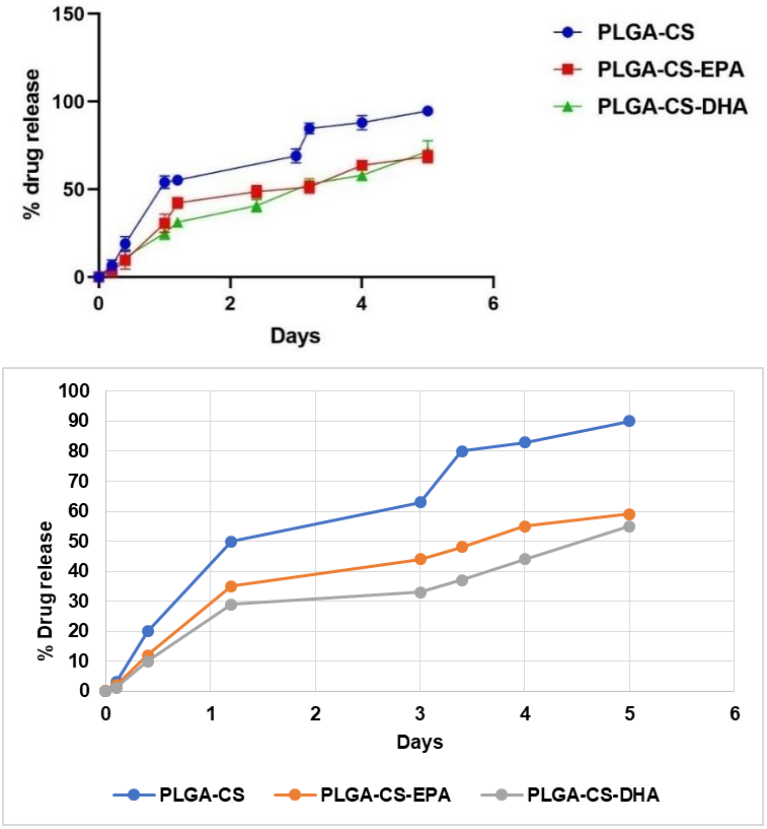

Fig. 8: *In vitro* drug release of (a) PLGA-CS (b) PLGA-CS-EPA (c) PLGA-CS-DHA, value are given in mean mean ±SD, n=3

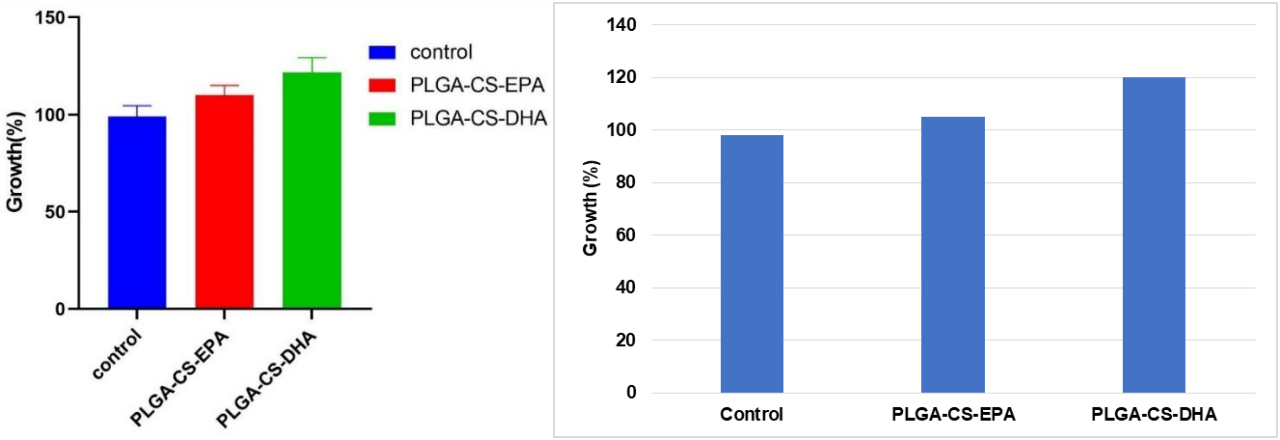

Fig. 9: MTT assay of the fibroblast 3T3-L1 Cell (negative control) and fibroblast cultured in the presence of placebo [PLGA-CS-EPA], [PLGA-CS-DHA]. Data was analyzed by applying two-way *ANOVA* with Tukey's posthoc test

MTT assay

In vitro cytotoxicity was performed on 3T3-L1 fibroblast cell lines. The cytotoxicity test revealed that the tested formulations didn't show any cytotoxic effects on cell lines. The crosslinked scaffolds induced cell growth, followed by non-crosslinked scaffolds (PLGA-CS), compared to the control group. The prepared scaffolds were biocompatible and increased cell growth due to the effect of EPA and DHA fatty acids on the scaffolds. Hence, prepared crosslinked and non-crosslinked scaffolds increase cell growth such that both the formulation aid in improving wound heal when compared with plain (fig. 9) [23].

CONCLUSION

In the present work, novel formulations containing PLGA-CS, PLGA-CS-EPA, and PLGA-CS-DHA were prepared, and these scaffolds were prepared using the electrospinning method. They were optimized using Box-Behnken design using design expert software. These scaffolds were crosslinked with EPA and DHA, increasing porosity and good water absorption ratio when compared to non-crosslinked. Further FTIR study revealed they were compatible with each excipients used. SEM results indicated they showed good porosity between spaces and accumulated drugs in their size. *In vitro* drug release showed crosslinked scaffolds with initial burst release followed by a sustained release pattern. *In vitro* cytotoxicity studies proved that cell growth occurred in crosslinked scaffolds. Hence, this novel formulation could aid in treating diabetic wounds better.

ACKNOWLEDGEMENT

The authors would like to thank the Department of Science and Technology-Fund for Improvement of Science and Technology Infrastructure (DST-FIST), Promotion of University Research and Scientific Excellence (DST-PURSE) for the facilities provided for conducting the research.

FUNDING

No funding was received for this work.

AUTHORS CONTRIBUTIONS

Shilpa. N. Thumbooru-Conceptualization, validation, Methodology, Writing–Original Draft Preparation and Data curation. Syed Suhaib Ahmed-Data curation, methodology, Writing–Review and Editing. Balaji Hari-Data curation, Writing–Review and Editing. Karri VVS Narayana Reddy–Conceptualization, Formal Analysis, validation, and Supervision.

CONFLICT OF INTERESTS

There is no conflict of interest

REFERENCES

1. Williams R, Karuranga S, Malanda B, Saeedi P, Basit A, Besancon S. Global and regional estimates and projections of diabetes-related health expenditure: results from the international diabetes federation diabetes atlas 9th edition. Diabetes Res Clin Pract. 9th Ed. 2020 Apr 1;162:108072. doi: 10.1016/j.diabres.2020.108072, PMID 32061820.
2. Siersma V, Thorsen H, Holstein PE, Kars M, Apelqvist J, Jude EB. Health-related quality of life predicts major amputation and death but not healing in people with diabetes presenting with foot ulcers: the eurodiale study. Diabetes Care. 2014;37(3):694-700. doi: 10.2337/dc13-1212, PMID 24170755.
3. Morimoto M, Lee EY, Zhang X, Inaba Y, Inoue H, Ogawa M. Eicosapentaenoic acid ameliorates hyperglycemia in high-fat diet sensitive diabetes mice in conjunction with restoration of hypoadiponectinemia. Nutr Diabetes. 2016;6(6):e213. doi: 10.1038/nutd.2016.21, PMID 27348201.
4. Qin L, Mei Y, An C, Ning R, Zhang H. Docosahexaenoic acid administration improves diabetes-induced cardiac fibrosis through enhancing fatty acid oxidation in cardiac fibroblast. J Nutr Biochem. 2023;113:109244. doi: 10.1016/j.jnutbio.2022.109244, PMID 36470335.
5. Panda BP, Krishnamoorthy R, Bhattamisra SK, Shivashekaregowda NK, Seng LB, Patnaik S. Fabrication of second generation smarter PLGA based nanocrystal carriers for improvement of drug delivery and therapeutic efficacy of gliclazide in type-2 diabetes rat model. Sci Rep. 2019;9(1):17331. doi: 10.1038/s41598-019-53996-4, PMID 31758056.
6. Panda BP, Krishnamoorthy R, Shivashekaregowda NK, Patnaik S. Influence of poloxamer 188 on design and development of second-generation PLGA nanocrystals of metformin hydrochloride. Nano Biomed Eng. 2018;10(4):334-43. doi: 10.5101/nbe.v10i4.p334-343.
7. Sanapalli BK, Yele V, Singh MK, Thumbooru SN, Parvathaneni M, Karri VV. Human beta defensin-2 loaded PLGA nanoparticles impregnated in collagen chitosan composite scaffold for the management of diabetic wounds. Biomed Pharmacother. 2023;161:114540. doi: 10.1016/j.biopha.2023.114540, PMID 36934557.
8. Ahmed SS, Baqi MA, Baba MZ, Jawahar N. Formulation characterization and optimization of folic acid tailored daidzein solid lipid nanoparticles for the improved cytotoxicity against colon cancer cells. Int J App Pharm. 2024 Mar;16(2):320-8. doi: 10.22159/ijap.2024v16i2.49879.
9. Natarajan J, Sanapalli BK, Bano M, Singh SK, Gulati M, Karri VV. Nanostructured lipid carriers of pioglitazone loaded collagen/chitosan composite scaffold for diabetic wound healing. Adv Wound Care. 2019 Oct 1;8(10):499-513. doi: 10.1089/wound.2018.0831, PMID 31737408.
10. Mat Saad AZ, Khoo TL, Halim AS. Wound bed preparation for chronic diabetic foot ulcers. ISRN Endocrinol. 2013;2013(1):608313. doi: 10.1155/2013/608313, PMID 23476800.
11. Ahmed SS, Sriramcharan P, Arivuselam R, Raman R, Venkatachalam S, Natarajan J. Green synthesis of bovine serum albumin tailored silver nanoparticles from *aspergillus fumigatus*: statistical optimization characterization antioxidant and cytotoxicity evaluation on colon cancer cells. Applied Organom Chemis. 2024 Apr;38(4):e7386. doi: 10.1002/aoc.7386.
12. Hu X, He J, Qiao L, Wang C, Wang Y, Yu R. Multifunctional dual network hydrogel loaded with novel tea polyphenol magnesium nanoparticles accelerates wound repair of MRSA infected diabetes. Adv Funct Materials. 2024 Feb 6;34(22):2312140. doi: 10.1002/adfm.202312140.
13. Sharma A, Mehta V, Parashar A, Patrwal R, Malairaman U. Solid lipid nanoparticle: fabricated through nanoprecipitation and their physicochemical characterization. Int J Pharm Pharm Sci. 2016 Aug 12;8(10):144. doi: 10.22159/ijpps.2016v8i10.13207.
14. Varma R, Vasudevan S. Extraction characterization and antimicrobial activity of chitosan from horse mussel *modiolus Modiolus*. ACS Omega. 2020 Aug 18;5(32):20224-30. doi: 10.1021/acsomega.0c01903, PMID 32832775.
15. Mahalingam M, Krishnamoorthy K. Camptothecin loaded poly (meth acyclic acid-co-methyl-methyacrylate) nanoparticles: fabrication characterization and cytotoxicity studies. Int J Pharm Pharm Sci. 2015;7(10):135-40.
16. Chen Y, Zhao W, Dai H. Porous PLGA-PEG nerve conduit decorated with oriented electrospun chitosan RGD nanofibre. J Mater Res Technol. 2021 Nov 1;15:86-98. doi: 10.1016/j.jmrt.2021.07.117.
17. Montanheiro TL, Montagna LS, Patrulea V, Jordan O, Borchard G, Ribas RG. Enhanced water uptake of PHBV scaffolds with functionalized cellulose nanocrystals. Polym Test. 2019;79:106079. doi: 10.1016/j.polymertesting.2019.106079.
18. Rajput IB, Tareen FK, Khan AU, Ahmed N, Khan MF, Shah KU. Fabrication and in vitro evaluation of chitosan gelatin-based aceclofenac loaded scaffold. Int J Biol Macromol. 2023 Jan 1;224:223-32. doi: 10.1016/j.ijbiomac.2022.10.118, PMID 36265543.
19. Intini C, Elviri L, Cabral J, Mros S, Bergonzi C, Bianchera A. 3D-printed chitosan-based scaffolds: an in vitro study of human skin cell growth and an in vivo wound healing evaluation in experimental diabetes in rats. Carbohydr Polym. 2018 Nov 1;199:593-602. doi: 10.1016/j.carbpol.2018.07.057, PMID 30143167.
20. Jahangir MA, Khan R, Sarim Imam S. Formulation of sitagliptin loaded oral polymeric nano scaffold: process parameters evaluation and enhanced antidiabetic performance. Artif Cells Nanomed Biotechnol. 2018 Oct 31;46 Suppl 1:66-78. doi: 10.1080/21691401.2017.1411933, PMID 29226729.

21. Khazaeli P, Alaei M, Khaksarihadad M, Ranjbar M. Preparation of PLA/chitosan nanoscaffolds containing cod liver oil and experimental diabetic wound healing in male rats study. J Nanobiotechnology. 2020 Dec;18(1):176. doi: 10.1186/s12951-020-00737-9, PMID 33256764.
22. Bhardwaj A, Modi KP. Antidiabetic and antihyperlipidaemic activity of nelumbo nucifera gaertn ethanol seed extract in streptozotocin-induced diabetic rats. Int J Pharm Pharm Sci. 2017;9(10):197. doi: 10.22159/ijpps.2017v9i10.21455.
23. Anitha R, Vaikkath D, Shenoy SJ, Nair PD. Tissue-engineered islet like cell clusters generated from adipose tissue-derived stem cells on three-dimensional electrospun scaffolds can reverse diabetes in an experimental rat model and the role of porosity of scaffolds on cluster differentiation. J Biomed Mater Res A. 2020 Mar;108(3):749-59. doi: 10.1002/jbm.a.36854, PMID 31788956.